Edited by S. Selberherr, H. Stippel, E. Strasser – September 1993

Numerical Modeling and Simulation of Multi-Electrode Semiconductor Optical Amplifiers

J. L. Pleumeekers[‡†], T. Mercier[‡], S. Mottet[‡], and F. Clérot[‡]

[‡]CNET Lannion B, France Telecom
Route de Trégastel, BP 40, F-22301 Lannion Cédex, FRANCE
[†]Department of Electrical Engineering, TU Delft
Mekelweg 4, P.O. Box 5031, NL-2600 GA Delft, THE NETHERLANDS

Abstract

The purpose of our study was to build a two-dimensional time-dependent simulator for multi-electrode semiconductor optical amplifiers with bulk active layers. This simulator was used to design an InGaAsP-InP external modulator at 1.55 μm for fast optical fibre transmission applications.

1. Introduction

For optical fibre applications, a new generation of multifunctional devices, based on semiconductor optical amplifiers (SOAs), is arising. The main studied functions are optical amplification, modulation, detection and wavelength conversion. A main studied point is the capability of integration of different functions in one device. The integration leads to multielectrode devices. To study and design these devices, a time-dependent simulator for multielectrode multifunction SOA has been developped. An SOA has anti-reflection coatings, so the travelling wave approximation (no facet reflectivities) can be used. Moreover, its structure (fig. 1) permits to solve the optical problem only along the light propagation z-axis. On the other hand, the electrical problem has to be solved within the xz plane : the main conduction takes place in the x direction but inhomogeneities, due to the internal optical mode amplification and the different biases of the top electrodes, are present in the z-direction.

2. Equation set

The electrical and optical behaviour of SOAs is described by the following five equations:

Poisson equation:
$$\nabla\bullet\,(\varepsilon\cdot\nabla\,\varphi) = q\cdot(n-p-dop) \qquad (1)$$

Electron continuity equation:
$$\frac{\partial n}{\partial t}-\nabla\bullet\,(n\cdot\mu_n\cdot\nabla\,\varphi_n) = -U(I) \qquad (2)$$

Hole continuity equation:
$$\frac{\partial p}{\partial t}+\nabla\bullet\,(p\cdot\mu_p\cdot\nabla\,\varphi_p) = -U(I) \qquad (3)$$

Light intensity propagation equation: $$\frac{1}{v_p} \cdot \frac{\partial I}{\partial t} + \frac{\partial I}{\partial z} = [\Gamma \cdot g(\varphi, \varphi_n, \varphi_p) - \alpha_s] \cdot I \quad (4)$$

Light phase propagation equation: $$\frac{1}{v_g} \cdot \frac{\partial \phi}{\partial t} + \frac{\partial \phi}{\partial z} = \alpha_H \cdot \Gamma \cdot g(\varphi, \varphi_n, \varphi_p) \quad (5)$$

where φ_n and φ_p are the Fermi-potentials, Γ is the optical confinement factor and α_H is the linewidth enhancement factor [1].

3. Solving method

After discretisation in time with a coefficient of implicitness θ [2], equations 1 to 3 can be written at time $t + \Delta t$ as:

$$\nabla \bullet (\varepsilon \cdot \nabla \varphi) = q \cdot (n - p - dop) \quad (6)$$

$$\nabla \bullet (n \cdot \mu_n \cdot \nabla \varphi_n) = U + \frac{n}{\theta \cdot \Delta t} - \frac{n^0}{\theta \cdot \Delta t} - \frac{1-\theta}{\theta} \cdot \nabla \bullet (n^0 \cdot \mu_n^0 \cdot \nabla \varphi_n^0) + \frac{1-\theta}{\theta} \cdot U^0 \quad (7)$$

$$\nabla \bullet (p \cdot \mu_p \cdot \nabla \varphi_p) = -U - \frac{p}{\theta \cdot \Delta t} + \frac{p^0}{\theta \cdot \Delta t} - \frac{1-\theta}{\theta} \cdot \nabla \bullet (p^0 \cdot \mu_p^0 \cdot \nabla \varphi_p^0) - \frac{1-\theta}{\theta} \cdot U^0 \quad (8)$$

where the superscript means the former solution at time t. These equations will be solved with as unknowns the potentials φ, φ_n and φ_p. They are all expressed in volt, so scaling or transformation of the variables is not necessary. The stationary solution is directly obtained by setting $1/\Delta t = 0$ and $\theta = 1$. Thus, the same solving method is used for both stationary and transient simulations. These equations are then discretised in a two-dimensional xz-space by a box method [3].

The optical equations, 4 and 5 , are solved only in the z-direction (decentred on the same mesh). The light intensity at time $t + \Delta t$ at mesh point i can be computed recursively after discretisation in time and z-space as:

$$I_i = \frac{\theta \cdot \frac{I_{i-1}}{H_{z_{i-1}}} + \frac{I_i^0}{v_p \cdot \Delta t} + (1-\theta) \cdot (\Gamma \cdot g_i^0 - \alpha_s) \cdot I_i^0 - (1-\theta) \cdot \frac{I_i^0 - I_{i-1}^0}{H_{z_{i-1}}}}{\frac{1}{v_p \cdot \Delta t} - \theta \cdot (\Gamma \cdot g_i - \alpha_s) + \frac{\theta}{H_{z_{i-1}}}} \quad (9)$$

where the superscript means the former solution at time t. The boundary condition is the incident light power I_0. In the same way, the light phase at time $t + \Delta t$ at mesh point i is computed as:

$$\phi_i = \frac{\theta \cdot \frac{\phi_{i-1}}{H_{z_{i-1}}} + \frac{\phi_i^0}{v_g \cdot \Delta t} + \theta \cdot \alpha_H \cdot \Gamma \cdot g_i - (1-\theta) \cdot \frac{\phi_i^0 - \phi_{i-1}^0}{H_{z_{i-1}}} + (1-\theta) \cdot \alpha_H \cdot \Gamma \cdot g_i^0}{\frac{1}{v_g \cdot \Delta t} + \frac{\theta}{H_{z_{i-1}}}} \quad (10)$$

The full set of equations is solved within a direct coupled Newton iterative scheme [4].

The SOAs are driven by modulated current sources, so transient current boundary conditions have to be implemented within the two-dimensional direct coupled

Newton method. This condition can be written for each contact as:

$$\sum_{nodes} (J_n + J_p + J_d) \bullet S_{box} = I_{bias} \tag{11}$$

where J_d is the displacement current density.

4. Applications

Among the different possible applications, the simulator was used to design an InGaAsP-InP external modulator at 1.55 µm for fast optical fibre transmission applications. It allows to access the internal and external behaviour of a SOA, under stationary and transient conditions together with the performances in system operation. As an example, the electron density is shown in figure 2 for an input power of -5 dBm and currents of 20 mA and 50 mA on the two contacts which gives a total optical gain of 11 dB. The inhomogeneity in the z-direction can be seen on that figure. One important parameter is the electrodes isolation under operation. The current density in the longitudinal z-direction for the etched region between the two contacts is shown in figure 3. It permits to evaluate the interelectrode leakage current under operation. This current appears in the active layer under operation, due to internal equilibrium and cannot be measured directly. It is a penalising effect which has to be taken into account for the design of the external current drivers. In figure 4 the optical output power time response is shown under current modulation of one of the electrodes. Owing to system performance requierements, the optimisations of the SOA showed that a counterphase current modulation [5] had to be used to obtain a fast modulation of the optical power together with an acceptable variation of the phase. The typical output power and phase under operation are shown in figure 5.

These two-dimensional transient simulations required a mesh of typically 3000 nodes together with 40 time steps.

References

[1] C.H. Henry, "Theory of the Linewidth of Semiconductor Lasers," IEEE J. Quantum Electron., Vol. QE-18, No. 2, pp. 259-264, 1982.

[2] J.E. Viallet and S. Mottet, "Transient Simulation of Heterostructures," NASECODE IV Conf., J.J.H. Miller (Ed.), Boole Press, Dublin, pp. 536-542, 1985.

[3] C. Simon, S. Mottet and J.E. Viallet, "Autoadaptive Mesh Refinement", SISDEP 1991, Vol. 4, W. Fichtner and D. Aemmer (Ed.), Hartung-Gorre, pp. 225-233, 1991.

[4] C. Simon, "Numerical Simulation of the Electronic Conduction in Semiconductor Devices: Discretisation and Auto-adaptive Meshing", Ph.D. thesis, university of Rennes, 1990.

[5] T.N. Nielsen, U. Gliese, T. Durhuus, K.E. Stubkjaer, B. Fernier, P. Garabedian, E. Derouin and F. Leblond, "Chirp-free 2.5 Gbit/s Amplitude Modulation / Gating in Two-electrode Semiconductor Optical Amplifiers", ECOC 1992.

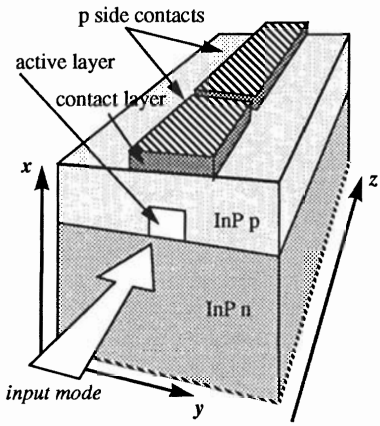

Figure 1: Sketch of a bielectrode SOA, with the different axes.

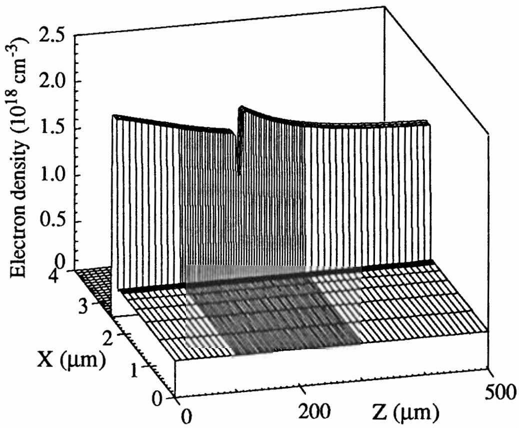

Figure 2: Electron density in the device. The inhomogeneity in the z-direction is clearly seen.

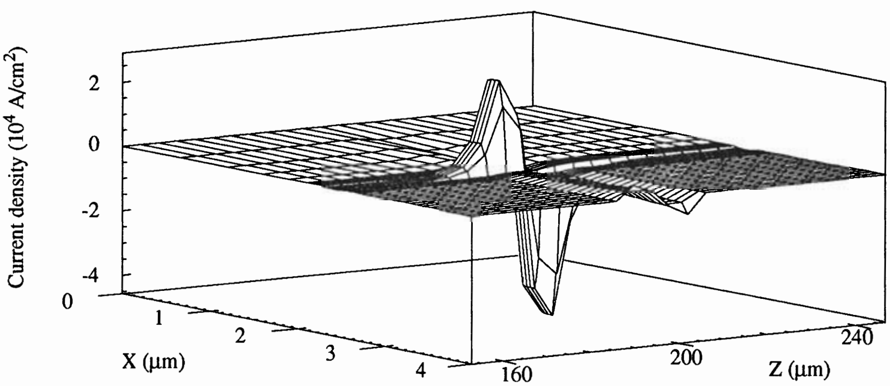

Figure 3: The z-component of the current density vector.

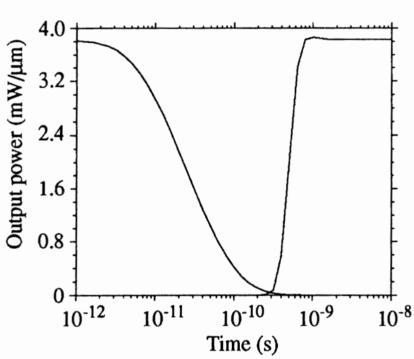

Figure 4: The optical response of the device.

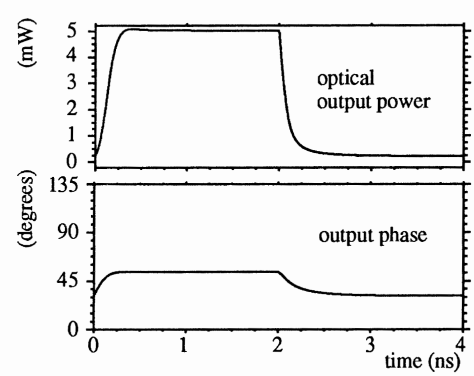

Figure 5: The optical response of the device under counterphase modulation of the electrodes.